International Journal of ISSI, Vol.3 (2006), No. 1, pp. 1-7

The Strain Dependence of Post-Deformation Softening during the Hot Deformation of 304H Stainless Steel

A. Najafizadeh[1*] and J. J. Jonas[2]
1- Department of Materials Engineering, Isfahan University of Technology, Isfahan, Iran
2- Department of Metallurgical Engineering McGill University, Montréal, Canada
Received August 6, 2006; Accepted November 4, 2006

Abstract
Experiments were carried out in which the dependence of the fractional softening on temperature, time and strain rate was determined in a 304H stainless steel. Three prestrain ranges were identified pertaining to three different post-deformation softening behaviors: 1) prestraining to below the DRX critical strain: strongly strain dependent softening by SRX alone with softening kinetics controlled by growth rate of the nuclei; 2) prestraining to above the DRX critical strain: SRX + MDRX softening with weaker strain dependence of the kinetics but still controlled by grain growth; 3) at a prestrain of ε* and beyond: nucleation-controlled MDRX softening with the full inhibition of SRX. The transition prestrain ε* can exceed the peak strain if the DRX grain refinement ratio $g = D_0/D_{DRX} > 4$.
The transition to MDRX-dominated softening can be attributed to a constant value of the normalized strain hardening rate independent of the preloading temperature and strain rate. The softening data from the compression tests show that at ε*, the time for half softening t_{50} exhibits a minimum. These data differ somewhat from observations obtained in the torsion testing of solid bars, in which no strain dependence of t_{50} was detected at ε* and beyond. Whether or not the strain dependence of t_{50} vanishes in the MDRX range is sensitive to the test method employed to study the post-deformation softening.

Keywords: Hot deformation, 304H stainless steel, Metadynamic recrystallization, Softening kinetics

Introduction

Austenitic stainless steels are known to be hard-to-deform in industrial multipass hot working. This is not only because of their relatively high deformation resistance but, also because of slow interpass softening due to sluggish diffusion induced by the high alloy content. A thorough understanding of interpass softening at elevated temperatures is important for high quality manufacturing of these steels, especially for those processing routes that induce large thermal, deformation and strain rate gradients in a workpiece.

On the other hand, austenitic stainless steels are convenient materials for the laboratory study of post-deformation softening. First, there is the possibility of microstructural evaluation after direct quenching from high temperatures, as these steels do not undergo phase transformation upon cooling. Furthermore, slow softening allows for wide ranges of post-deformation holding times without the risk of complete softening, as in other steels with leaner alloying additions.

* *Corresponding author:*
Tel:+98-311-3915742 Fax: +98-311-3912752
E-mail: A-najafi@cc.iut.ac.ir
Address: Dept. of Materials Engineering,
Isfahan University of Technology, Isfahan, 8415683111, IRAN

It is widely accepted that two recrystallization mechanisms operate during interpass intervals in hot working. First, at relatively high temperatures, there is conventional static recrystallization (SRX)[1-3], which involves the nucleation and growth of dislocation-free grains, that is, grains with dislocation densities several orders of magnitude lower than in the deformed matrix.

The initiation of SRX requires a certain amount of static recovery beforehand (the incubation period), which can contribute to measurable softening[1-2]. At relatively low temperatures (below the no-recrystallization temperature T_{nr} for SRX), softening occurs by metadynamic recrystallization (MDRX) if dynamic recrystallization (DRX) has taken place during the preceding deformation. As opposed to SRX, MDRX involves only the *growth* of dynamically recrystallized grains. At temperatures above T_{nr}, both SRX and MDRX can operate simultaneously in different parts of the material if the preceding deformation has been sufficient to initiate DRX; in this case, the dynamically recrystallized grains grow as a result of MDRX, while SRX can occur in the regions that have not undergone DRX. It has been proposed that under these conditions MDRX is significantly more rapid than SRX since the former does not seem to require an incubation time[4-6].

Softening kinetics are generally quantified in terms of the time for half (50%) softening t_{50} or in

terms of the rate constant that is inversely proportional to t_{50}. Regardless of material chemistry, the kinetics of SRX (namely, t_{50}) are known to exhibit fairly weak strain rate dependence but are strongly influenced by the preloading strain and quite sensitive to temperature due to the relatively high activation energy[7-9]. By contrast, MDRX depends only weakly on the preceding strain and has a somewhat lower activation energy; concurrently, it is much more strain rate sensitive[7-11]. Within certain ranges of processing conditions, there can be a gradual transition from SRX- to MDRX-dominated softening.

The objective of the present work was to analyze the interpass softening behavior of a typical austenitic stainless steel under conditions where both types of post-deformation recrystallization take place and especially to address the effects of the preloading conditions on the strain dependence of post-deformation softening.

Experimental Procedures

The present work concerned a 304H stainless steel (wt%: 0.067 C, 1.74 Mn, 0.71 Si, 17.65 Cr, 7.91 Ni, 0.57 Mo, and 0.32 Cu). The material was supplied in the form of a hot rolled bar with a diameter of 7.94 mm. Cylindrical specimens 7.9 mm in diameter and 11.5 mm in height were prepared with their axes parallel to the rolling direction.

One- and two-hit constant strain rate isothermal hot compression tests were carried out on a computer-controlled servo-hydraulic MTS machine equipped with a radiant furnace. Prior to deformation, the specimens were preheated at 1200°C for 15 min, then cooled to the test temperature at 1°C/s and held for 5 min for temperature homogenization. An argon atmosphere was provided throughout the entire thermal cycle. Mica plates covered with boron nitride powder were used to minimize friction during hot compression. The tests were run at 900 – 1100 °C and strain rates of 0.01 – 1 sec^{-1}. Single hit tests were performed to a strain of 1, while in the double-hit tests the strains of the first hit were varied as described below. Interpass times ranged from 0.3 to 1000 sec. The fractional softening was determined using the 1% offset stress method.

Results and Discussion

Representative single-hit (continuous) flow curves are illustrated in Figure 1. The curves exhibit stress peaks and subsequent softening to a steady state indicative of DRX behavior. It has recently been shown[8,12-13] that laboratory simulations of interpass softening can be considerably simplified if the normalized strain $w = \varepsilon/\varepsilon_p$ is kept constant instead of the pass strain ε, where ε_p is the peak strain. Under these conditions, although the pass strains change with strain rate and temperature, the log $t_{50} - w$ plots have similar shapes[12], which significantly simplifies analysis of the post-deformation softening behavior.

From the continuous flow curves, the following characteristic strains were selected for preloading in the double-hit tests (Figure 2): the critical strain for the initiation of DRX (ε_c); the peak strain (ε_p); the strain ε_i at the point of inflection of the flow curve beyond the stress peak; the strain corresponding to the onset of steady state flow (ε_s). The critical strains ε_c were determined using the method of Ref. [14] from the point of inflection in the strain hardening rate (θ) *vs* flow stress (σ) plot. This way the critical stress was determined and then the value of ε_c was obtained from the initial flow curve.

The strains ε_i were identified as those corresponding to the maximum absolute value of θ beyond the stress peak. In addition, preloading to strains of $\frac{1}{2}(\varepsilon_c + \varepsilon_p)$ was used. In the tests, the respective normalized strains w_c, $w_p = 1$, w_i, etc., were kept fixed so that the first hit strains differed for different test temperatures and strain rates.

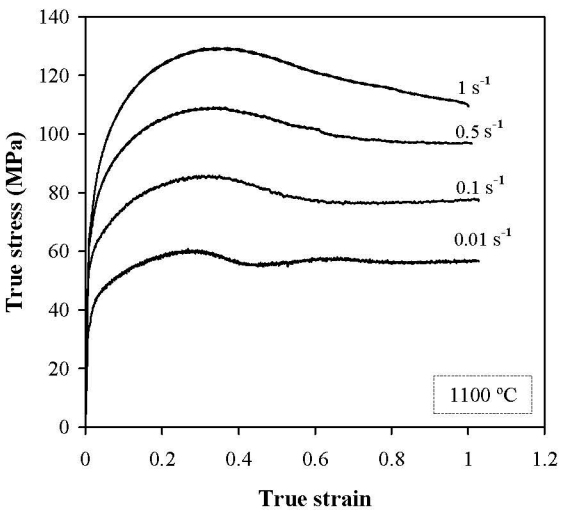

Fig. 1. Typical 304H single hit compression flow curves.

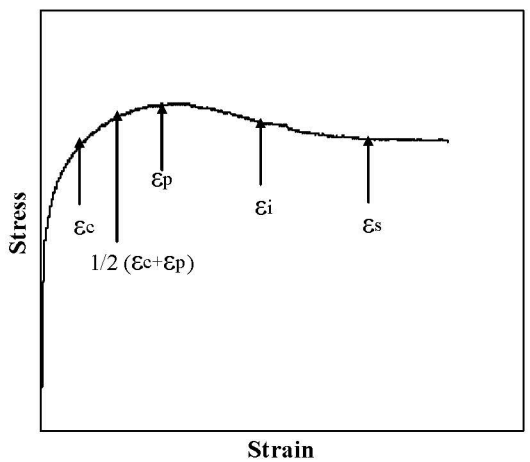

Fig. 2. Characteristic strains selected for preloading in the double-hit tests.

The dependences of the fractional softening on temperature and prestrain are illustrated by the softening curves presented in Figures 3 and 4. All of the softening curves are S-shaped and do not display any plateaus. As expected, the fractional softening increases with increasing temperature, strain rate and strain for a given post-deformation holding time.

The time for 50% softening decreases with prestrain when the latter increases from ε_c to ε_i, Figures 3 and 4. After prestrains greater than ε_i, t_{50} becomes less strain dependent than after smaller prestrains.

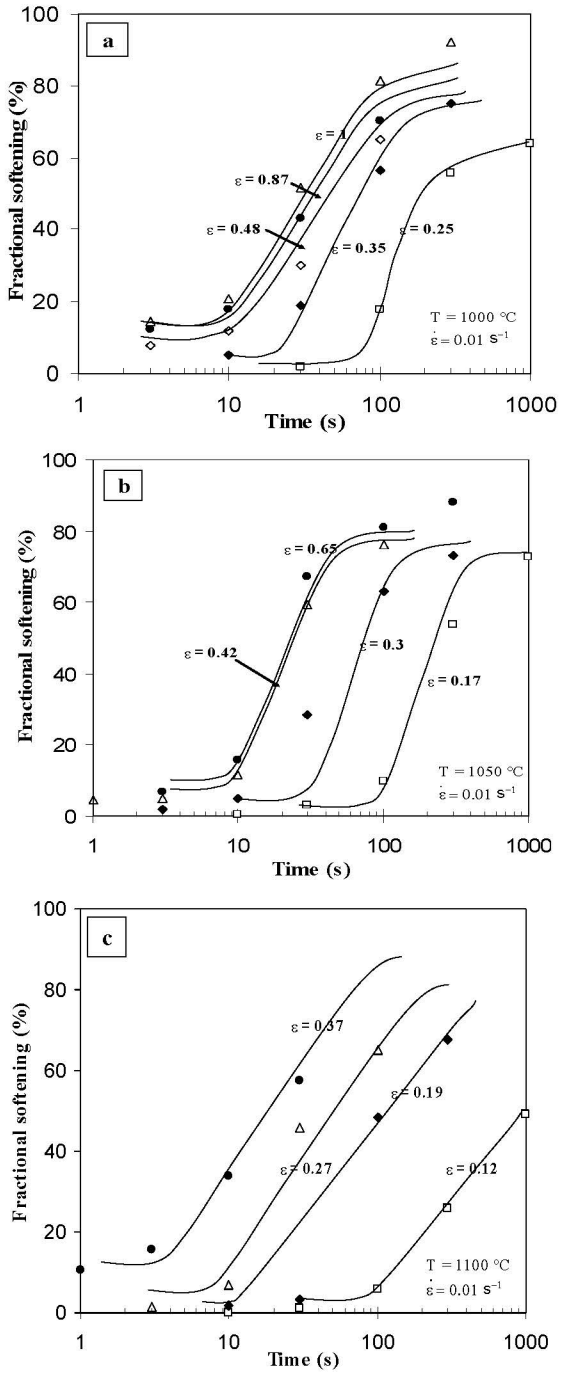

Fig. 3. Evolution of fractional softening with time and prestrain at 0.01 sec^{-1} and (a) 1000°C, (b) 1050°C and (c) 1100°C.

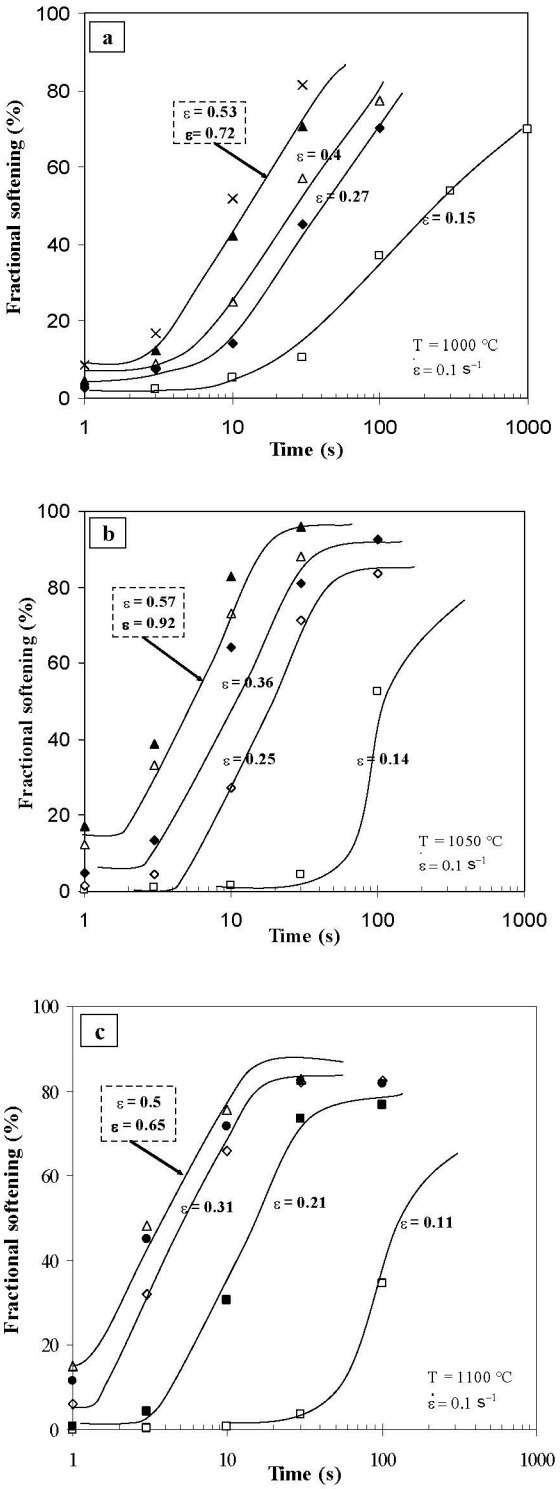

Fig. 4. Evolution of fractional softening with time and prestrain at 0.1 sec^{-1} and (a) 1000°C, (b) 1050°C and (c) 1100°C.

Effect of Normalized Strain: To compensate for the effects of preloading strain rate and temperature, it is convenient to normalize the time required to attain various extents of softening t_F (F = 20, 50, 75 %) by the time for half softening after preloading to stress peak, t_{50}^p. Softening fractions of 20 and 75 % were selected because in

most of the cases considered here, they reliably represent the lower and upper boundaries of the linear portions of the softening curves (*cf.* Figures 3 and 4); that is, they describe the range of validity of the JMAK equation. Fig. 5 displays plots of the normalized softening time, log (t_F/t_{50}^P), against the normalized strain $w = \varepsilon/\varepsilon_p$. These plots readily reveal the following:

At prestrains around the DRX critical strain ($w \approx 0.48$), a large scatter of normalized t_{20} times can be observed. For greater extents of softening, the scatter is much smaller but strong strain dependence (more precisely, w-dependence) can be noted. With increasing prestrain, the w-dependences of t_{50} and t_{75} become weaker and close to that of t_{20}: the slopes $d\log (t_F/t_{50}^P)/dw$ are similar and independent of the softening fraction F. After large prestrains ($w \approx 1.33$), t_{50} and t_{75} attain a sort of minimum while t_{20} does not.

At very high prestrains close to the onset of the steady state ($w \approx 1.8$), a slight increase in t_{50} and t_{70} can be noted, as opposed to t_{20}, which keeps on decreasing with w at a constant slope. A similar trend of increasing t_{50} at high prestrains during the compression of C – Mn steels has been reported in the literature (see [12, 15]).

Thus, three regions can be identified in Fig. 5 that differ in terms of the slope in the log (t_F/t_{50}^P) *vs* w plots: region I with a very high (negative) slope, region II with a somewhat lower slope, and region III where the slope $d\log(t_F/t_{50}^P)/dw$ changes its sign remaining, however, fairly small.

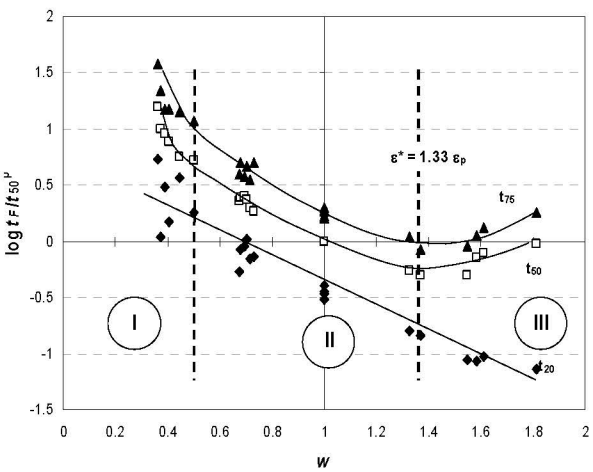

Fig. 5. Dependence of normalized softening time on normalized strain w.

Comparison with Torsion Testing Results: The above results somewhat resemble those obtained by Zahiri and Hodgson on medium carbon steel using torsion testing[4]. The authors of Ref. [4] identified four regions in their $\log t_F$ – ε plots: region I pertaining to softening by SRX only, which corresponds to prestrains below the DRX critical strain; region II for prestrains between ε_c and ε_p, where both the SRX and MDRX mechanisms are activated; region III for prestrains between ε_p and ε^*, also with softening by SRX + MDRX and the *same* slope $d\log t_{50}/d\varepsilon$ as in region II. Finally, there is region IV for prestrains to ε^* and above, where the strain dependence of t_{50} vanishes; the softening here occurs by MDRX only. Their plots differ from those in Fig. 5 in that the latter represent the normalized quantities. Such normalization would, in fact, eliminate the difference between regions II and III in [4] had the data there been normalized in the same way as in Figure 5.

Numerous observations of the abrupt change in the slope $d\log t_{50}/d\varepsilon$ at ε^*, beyond which t_{50} no longer depends on the strain have been reported in the literature from torsion testing. The results of Djaic and Jonas on high carbon steel[16] as well as those of Cho *et al.* on Nb microalloyed steel[8-9] show that abrupt changes in t_{50} can take place at strains of about ε_p. These authors attributed the abrupt transition from strain dependence to the strain independence of t_{50} at peak strains to the changes associated with MDRX becoming the dominant softening process.

Uranga *et al.*[17] reported that the strain-independent range for t_{50} begins at a prestrain of about $\varepsilon^* = 1.7\varepsilon p$ in a Nb microalloyed steel. Zahiri *et al.*[18] noted that the transition strain ε^* in IF steels is just above ε_p depending, however, on the Zener-Hollomon parameter Z pertaining to the preloading conditions. Other examples of sharp transitions in the strain independence of t_{50} determined by means of the *torsion* testing of solid bars can be found in Refs. [6 – 10, 19 – 22] but are not limited to these works.

Summarizing these observations, it can be concluded that although the transition prestrain ε^* is indicative of the significant spread of DRX and hence of MDRX, it can be higher than the peak strain but less than the strain required to attain steady state flow and complete DRX. That is, the attainment of strain independence for t_{50}, attributable to post-deformation softening solely by MDRX, and the completion of DRX during preloading does not occur at the same prestrain. In other words, when the strain dependence of t_{50} vanishes, a part of the preloaded material still remains that has not been touched by dynamic recrystallization and hence it is possible for SRX to occur there.

Interpreting the Differences Between the Compression and Torsion Testing Results: The softening data from *compression* tests, obtained in the present study as well as in other investigations, differ somewhat from the observations obtained in torsion testing. Instead of the strain dependence of t_{50} vanishing at ε^*, the t_{50} time exhibits a minimum at ε^* and then slowly increases up to the prestrain corresponding to the onset of steady state flow. It appears that whether or not the strain dependence of t_{50} vanishes in the MDRX range is sensitive to the test method employed to study the interpass softening. This must be closely related to the effect

of test method on the peak strain and especially on the strain for complete DRX (ε_s) during hot deformation[23-24].

It is particularly relevant to this discussion that the ratio ε_p(torsion)/ε_p(compression) is smaller than ε_s(torsion)/ε_s(compression) mostly because ε_s(torsion) >> ε_s(compression)[24]. This discrepancy stems from the large radial strain and strain rate (and hence stress) gradients inherent in the torsion testing of solid bars. As a result of these gradients, ε_p and ε_s are different in each concentric layer in the torsion specimen.

Recalling that the time required to attain a given extent of DRX in each concentric layer is progressively delayed with increasing distance from the outmost layer of the specimen towards its center, post-deformation softening will also be progressively delayed in time with respect to the outermost layer. In this way, the times t_{50} determined by the offset stress method in torsion will reflect the effects of averaging the strains, strain rates and stresses over the specimen cross-section. Under these conditions, the true extent of softening cannot be determined with accuracy nor can the strain dependence of t_{50}. The apparent disappearance of the strain dependence of t_{50} at ε^* during the torsion testing of solid bars therefore requires more detailed analysis.

Bearing in mind the differences between torsion and compression testing, the three behaviors in Figure 5 can be interpreted as follows: Region I pertaining to preloading up to the DRX critical strain (w_c) is analogous to that outlined in Ref. [4]. It corresponds to softening by SRX alone and involves the strong strain dependence of nucleation and the weak strain dependence of growth[25]. The softening kinetics here are therefore controlled by the growth rate of the nuclei, i.e. by the slowest process. The growth rate is limited as the number of available nuclei increases more quickly than their size until impingement occurs. The large scatter in the time required to attain a small fraction of softening is indicative of the considerable inhomogeneity of the microstructure at this stage.

Once DRX has begun during preloading beyond w_c, the number of SRX nuclei begins to decrease along with the volume fraction of the deformed matrix and grain boundary area available for the nucleation of SRX. At the same time, the number of DRX grains growing during unloading by the MDRX mechanism increases with w. The net number of nucleation sites available for SRX therefore progressively decreases with prestrain, thus weakening the strain dependence of softening. Nevertheless, SRX nuclei still play active roles and softening is still controlled by grain growth.

In this respect, the peak strain does not represent a particular point that separates two distinct behaviors. Region II in Figure 5 is therefore a gradual transition from SRX- to MDRX-dominated behavior and is analogous to *both* regions II and III in Ref. [4]. Finally, once DRX has progressed to a sufficient extent (ε^*), the nucleation of SRX in the remaining deformed matrix is arrested. The overall softening kinetics become nucleation-controlled due to the deficit of SRX nuclei and the DRX grains grow rapidly by the MDRX mechanism until impingement.

In concert with accumulated experience, the transition prestrain ε^* can be simply defined as the prestrain that signifies the attainment of a state of microstructure and dislocation substructure that completely inhibits the nucleation of SRX, so that MDRX becomes the dominant softening mechanism.

The Incubation Time for MDRX: The S-shapes of softening curves at short holding times after large prestrains (Figures 3 and 4), even when MDRX becomes the dominant mechanism, suggest that MDRX still requires some sort of incubation time before its rapid progress begins. This can be explained by the relatively high dislocation density in the DRX grains as compared to that within fresh SRX nuclei. Indeed, the average dislocation density in DRX grains must be related to the steady state flow stress σ_s as $\rho_{DRX} \sim \sigma_s^2$. The difference in dislocation density between DRX grains and the adjacent deformed matrix, and consequently the driving force for grain growth by MDRX, is not very large when the unloading time is short. The intensive growth of DRX grains after deformation requires more rapid recovery in the dynamically recrystallized grains than in the adjacent matrix.

The relatively slow softening at short unloading times may therefore reflect the competition between prestrain independent recovery in the DRX grains and prestrain dependent recovery in the deformed matrix (with the latter being responsible for SRX nucleation). When recovery in the matrix is not fast enough to induce the nucleation of SRX before rapid MDRX grain growth begins, the nucleation of SRX is arrested. This defines the amount of prestrain ε^* after which SRX nucleation becomes fully suppressed. This is also why the t_{20} time continues to exhibit a fairly strong strain dependence even after prestrains to ε^* and beyond.

Slowing of the MDRX kinetics at long post-deformation holding times has also been observed by Xu and Sakai in tensile tests[26]. In the present study, the slight increases in t_{50} and t_{75} reflect a decrease in the driving force for MDRX grain growth with time. At long post-deformation times, contributions to this driving force are made, on the one hand, by differences in dislocation density between adjacent DRX/MDRX grains due to Taylor factor differences during deformation, and on the other, by differences in grain boundary energy also between adjacent DRX/MDRX grains. These differences are reduced as DRX progresses during deformation.

A Criterion for ε^*: The minimum prestrain ε^* after which MDRX becomes the dominant post-deformation softening mechanism requires the

preceding DRX to progress to a certain minimum volume fraction, X^*_{DRX}. It can be assumed that X^*_{DRX} corresponds to the moment at which the specific grain boundary area enclosing the *deformed matrix* that has not yet undergone DRX becomes equal to the specific area of all the DRX grain boundaries. From this instant on, the nucleation of SRX is fully suppressed. Post-deformation recrystallization then nucleates entirely by DRX, as pointed out in Ref. [19].

The specific DRX grain boundary area is the ratio of the DRX volume fraction to the diameter of the DRX grains, $3X_{DRX}/D_{DRX}$, assuming that the DRX grains are of spherical shape. The specific area of the boundaries that enclose the deformed matrix is $3/[D_0(1 - X_{DRX})]$. Here, it is assumed that pancaking of the initial grains has by this time been mostly eliminated by DRX, so that the shapes of the remaining deformed matrix grains are also not far from spherical. These grain boundary areas are equal to each other when:

$$X^*_{DRX}\frac{3}{D_{DRX}} = \frac{3}{D_0\left(1 - X^*_{DRX}\right)} \tag{1}$$

which is equivalent to the following simple quadratic equation:

$X^*_{DRX}{}^2 - X^*_{DRX} + 1/g = 0$

where $g = D_0/D_{DRX}$ is the DRX grain refinement ratio. The above equation yields the solution:

$$X^*_{DRX} = 0.5 \pm 0.5\sqrt{1 - 4/g} \tag{2}$$

This solution is quite interesting. First, the roots are real only if $g \geq 4$. There is experimental evidence that X^*_{DRX} can be as low as 50 % at ε^*[27], i.e. when $g = 4$. When $g > 4$, the "minus sign" solutions describe very low values of X^*_{DRX} that *decrease* with increasing g. These solutions probably reflect the situation right after the first DRX necklace has been formed. Beyond this point, the nucleation rate for SRX changes, and so does the growth rate that is limited by the number of nuclei. The "plus sign" solutions lead to X^*_{DRX} values that *increase* from $X^*_{DRX} = 0.72$ at $g = 5$ to $X^*_{DRX} = 0.85$ at $g = 8$, and so forth. Here, the SRX mechanism no longer contributes to the nucleation of recrystallization in the deformed matrix. Such an increase in X^*_{DRX} with increasing g must require a progressively wider span of strain for DRX to attain X^*_{DRX}. Interestingly enough, these considerations agree quite well with the experimental $\varepsilon^*/\varepsilon_p$ *vs* D_{DRX}/D_0 (= $1/g$) plot of Ref. [19] and do not depend on material chemistry, as in [19].

Effect of the Normalized Work Hardening Rate: The dependence of the normalized softening time on normalized strain w illustrated in Figure 5 follows quite closely the dependence of the normalized strain hardening rate $\Theta = [\partial(\sigma/\sigma_p)/\partial w]_{T,\dot{\varepsilon}}$ on normalized strain displayed in Figure 6. Like the normalized strain, the normalized strain hardening rate Θ is independent of preloading strain rate and temperature and can be associated with the extent to which the material has approached the steady state in the course of deformation. From the similarity between the behaviors of t_{50}/t_{50}^P and Θ, the transition to MDRX-dominated softening can be attributed to the attainment of a constant value of Θ^*. The conventional strain hardening rate at the transition, θ^*, must depend on Z since

$$\theta = \left(\sigma_p/\varepsilon_p\right)\Theta \tag{3}$$

where σ_p and ε_p are Z-dependent. For the steel studied here, the power law for the peak stresses holds, $\sigma_p = AZ^m$, with $m \approx 0.16$ averaged over the range of deformation conditions studied. For the peak strains, the relation $\varepsilon_p = BD_0{}^bZ^k$ also holds, with $k_{average} \approx 0.17$. Since the values of m and k for the present steel are close, the strain hardening rate at the transition θ^*

$$\theta^* = \left(ABD_0^{-b}\Theta^*\right)Z^{m-k} \tag{4}$$

is almost independent of Z, as illustrated in Figure 7. In many other materials, $m < k$, so that the absolute value of the strain hardening rate at the transition θ^* should decrease with Z. That is, as Z is increased, the prestrain required for the transition to MDRX-dominated softening will approach the onset of steady state flow. This conclusion is consistent with the effect of the DRX grain refinement ratio described above since the latter increases with increasing Z due to the decreasing value of D_{DRX}.

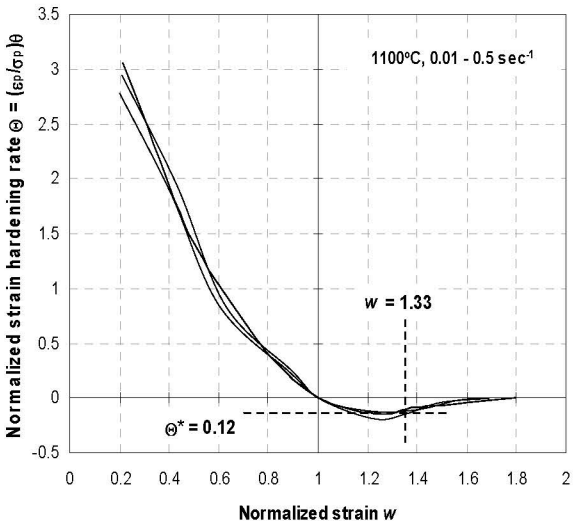

Fig. 6. Dependence of the normalized strain hardening rate on normalized strain.

Conclusions

Using the normalization of t_{50} and of the preloading strain, three prestrain ranges were identified pertaining to three different post-deformation softening behaviors:

1- Prestraining to below the DRX critical strain: strongly strain-dependent softening by SRX alone with the softening kinetics controlled by growth rate of the nuclei;
2- Prestraining to above the DRX critical strain: SRX + MDRX softening with weaker strain-dependence of the kinetics but still controlled by grain growth;
3- At the transition prestrain of ε* and beyond: nucleation-controlled softening by MDRX only with the full inhibition of SRX. Here, the DRX grains grow rapidly by the MDRX mechanism until impingement.

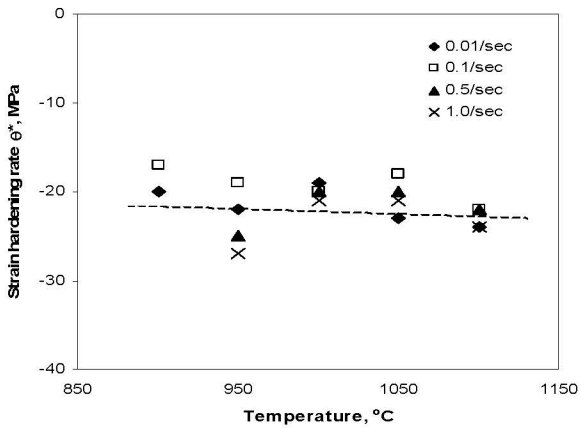

Fig. 7. Effects of temperature and strain rate on strain hardening rate θ^*.

The softening data from compression tests show that at a prestrain of ε*, the time for half softening t_{50} exhibits a minimum. These data differ somewhat from the observations obtained in the torsion testing of solid bars, where no strain dependence of t_{50} was detected at ε* and beyond. It appears that whether or not the strain dependence of t_{50} vanishes in the MDRX range is sensitive to the test method employed to study the post-deformation softening.

The prestrain ε* can exceed the peak strain if the DRX grain refinement ratio $g = D_0/D_{DRX} > 4$. The transition to MDRX-dominated softening can be attributed to a constant value of the normalized strain hardening rate that is independent of the preloading temperature and strain rate.

References

[1] C. M. Sellars: Mater. Sci Technol., 6 (1990), 1072.
[2] G. Li, T. M. Maccagno, D. Q. Bai, and J. J. Jonas: ISIJ Int., 36 (1996), 1479.
[3] H. L. Andrade, M. G. Akben, and J. J. Jonas: Metall. Trans. A, 14A (1983), 1967.
[4] S. H. Zahiri and P. D. Hodgson: Mater. Sci. Technol., 20 (2004), 458.
[5] J. J. Jonas: Mat. Sci. Eng. A, 184 (1994), 155.
[6] C. Roucoules and P. D. Hodgson: Mater. Sci. Technol., 11 (1995), 548.
[7] C. Roucoules, P. D. Hodgson, S. Yue, and J. J. Jonas: Metall. Mater. Trans. A, 25A (1994), 389.
[8] S. H. Cho, K. B. Kang and J. J. Jonas: ISIJ Int., 41 (2001), 766.
[9] S. H. Cho, K. B. Kang and J. J. Jonas: Mater. Sci. Technol., 18 (2002), 389.
[10] P. D. Hodgson: Mat. Sci. Technol., 12 (1996), 788.
[11] L. P. Karjalainen, T. M. Maccagno, and J. J. Jonas: ISIJ Int., 35 (1995), 1523.
[12] E. I. Poliak and J. J. Jonas: ISIJ Int., 44 (2004) 1874.
[13] J. J. Jonas and E. I. Poliak: Mater. Sci. Forum, 426-432 (203), 57.
[14] E. I. Poliak and J. J. Jonas: Acta mater., 44 (1996), 127.
[15] L. P. Karjalainen and J. Perttula: ISIJ Int., 36 (1996), 729.
[16] R. A. P. Djaic and J. J. Jonas: Metall. Trans., 4 (1973), 621.
[17] P. Uranga, A. I. Fernandez, B. Lopez, and J. M. Rodriguez- Ibabe: Mater. Sci. Eng. A, A345 (2003), 319.
[18] S. H. Zahiri, S. M. Byon, S. -I. Kim, Y. Lee, and P. D. Hodgson: ISIJ Int., 44 (2004), 1918.
[19] M. R. Cartmill, M. R. Barnett, S. H. Zahiri, and P. D. Hodgson: ISIJ Int., 45 (2005), 1224.
[20] A. I. Fernandez, B. Lopez, and J. M. Rodriguez - Ibabe: Mater. Sci. Forum, 467-470 (2004), 1169.
[21] J. M. Rodriguez-Ibabe: Mater. Sci. Forum, 500-501 (2005), 49.
[22] P. D. Hodgson, S. H. Zahiri, and J. J. Whale: ISIJ Int., 44 (2004), 1224.
[23] I. Weiss, T. Sakai, and J. J. Jonas: Metal Sci., 18 (1984) 77.
[24] T. Sakai and J. J. Jonas: Acta Metall., 32 (1984), 189.
[25] F.J. Humphreys and M. Hatherly: Recrystallization and Related Annealing Phenomena, (Elsevier Science, Oxford, 1995) 177, 188.
[26] Z. Xu and T. Sakai: Mater. Trans JIM, 32 (1991), 174.
[27] G. R. Stewart and A. M. Elwazri, private communication (2005).